

A Mirror encoding combined with the FFT for a fast heuristic of the RNA folding dynamics

Vaitea Opuu¹, Nono S. C. Merleau¹, and Matteo Smerlak¹

¹Max Planck Institute for Mathematics in the Sciences, D-04103 Leipzig, Germany

March 28, 2021

1 Abstract

- Simple and fast heuristic for the folding path of RNAs.
- It is straightforward to model Pseudoknots
- It's performance is comparable to exact method on the RNA folding problem
- It follows a simple idea which naively corresponds to RNA folds mechanism (many BPs formed at once to compensate for the lost of entropy)
- Among the 50 predicted structures, in average, at least one has pvv $\sim 74\%$ and sensitivity $\sim 76\%$.
- We propose a fast algorithm method based on the FFT to search for high density BP regions.
- There are smooth coarse-grain folding path which lead to near native structures.

2 Introduction

2.1 RNA folding introduction

bla bla dynamic of secondary structure relevant bla biological function.

- MFE and MEA not significantly different in term of performances (how to bench RNA)

2.2 RNA folding dynamics

1. Description of RNA structure
2. going up to the 2ndary structure only
3. Simple rules to compute a structure: multiple BPs compensate the lost of entropy during the folding process.

2.3 Energy model

1. issue with additivity principle in model. Might be worst when the sequence lengthens since more tertiary interactions interplay.

2.4 Existing methods

1. MC sampling: kinfold; atomic moves; MC-style simulation
2. Barrier trees from conformation landscape subopt tree: Sample from the boltzmann ensemble of structures
3. Vfold, simplified folding model

3 FFT based folding dynamic heuristic

We now describe the heuristic folding algorithm starting from one sequence S and its associated unfolded structure of length L . We first create a numerical representation of S where each type of nucleotide is replaced by a unit vector of 4 components:

$$A \rightarrow (1000) \ U \rightarrow (0001) \ C \rightarrow (0100) \ G \rightarrow (0010) \quad (1)$$

which gives us a $4 \times L$ matrix we call X where each row is a nucleotide type channel. Here, the first row would be the A channel which we refer to as X^A . Then, we create a second copy for which we revert the order of the sequence and use the following complementary encoding:

$$\bar{A} \rightarrow (000w_{AU}) \ \bar{U} \rightarrow (w_{AU}w_{GU}00) \ \bar{C} \rightarrow (00w_{GC}0) \ \bar{G} \rightarrow (0w_{GC}0w_{GU}) \quad (2)$$

where w_{AU} , w_{GC} , w_{GU} are tunable parameters for the next step. We call this new copy, the mirror of X .

For each of the 4 components, we compute the correlation between X and \bar{X} and simply sum up the four channels to obtain the correlation between the two copies:

$$cor(k) = (c_{X^A, \bar{X}^A}(k) + c_{X^U, \bar{X}^U}(k) + c_{X^G, \bar{X}^G}(k) + c_{X^C, \bar{X}^C}(k)) / \min(k, 2 \times L - k) \quad (3)$$

where $c_{X^A, \bar{X}^A}(k)$ is the correlation in the A channel between the two copies. The correlation $cor(k)$ gives the average number of base pairs for a positional lag k . One channel correlation between the copies is given by:

$$c_{X^A, \bar{X}^A}(k) = \sum_{1 \leq i \leq L, 1 \leq i+k \leq M} X^A(i) \times \bar{X}^A(i+k) \quad (4)$$

where $X^A(i)$ and $\bar{X}^A(i+k)$ are the A channel of site i and $i+k$. $X^A(i) \times \bar{X}^A(i+k)$ is non zero if sites i and $i+k$ can form a base pair, and will be the value of the chosen weight as described above. Although this operation requires $O(N^2)$ operation, it can take advantage of the FFT which reduces drastically its complexity to $O(N \log(N))$.

The large correlation values between the two copies indicates the positional lag between at which the base pair density is high. Therefore, we use a sliding window strategy to search for the longest consecutive base pairs within the positional lag. Since the copies are symmetrical, we only need to slide over one half of the positional lag. Once the longest base pairs are identified, we simply compute the free energy change when those base pair are formed. We perform the same search for the n highest correlation lags, which gives us n possible possibilities. Then, we added to the current structure the base pairs that gives the best change of energy.

We are now left with two segments, the interior and exterior of the group of consecutive base pairs formed. The two exterior fragments are concatenated together. Then, we simply apply recursively the same procedure on the two segments separately in a "Breath First" fashion to form new consecutive base pairs, until no base pair formation can improve the energy. However, it is straightforward to consider pseudoknots by simply concatenating all the fragments left.

The algorithm described so far tends to be stuck in the first local minima found along the folding trajectory. To alleviate this, we propose a stacking procedure where the 50 best trajectories are stored in a stack and evolved in parallel. Hence, it offers the flexibility of overcoming some energy barriers. **Figure** shows the whole procedure.

4 Folding RNAs

To evaluate the relevance of the folding model, we compared the algorithm performance for the folding task. In addition, to assess the effect of sequence lengths on these predictions, we displayed their performance length-wise.

Figure shows the performance in PPV and sensitivity for the four methods. It shows that the ML method is consistently better than thermodynamic methods. Length-wise T-test between the MFE and ML predictions showed that this difference is significant ($p\text{value} \approx 10^{-12}$) with a substantial improvement of about 10%. Although RAFFT predictions were found to be comparable to MFE predictions, they are significantly less accurate ($p\text{value} \approx 0.0002$), with a drastic loss of performance for sequences of length greater than 300 nucleotides.

Among the 50 configurations produced by RAFFT, we found in average at least one prediction with in average 59% of PPV and $\langle \text{SENS} \rangle$ of sensitivity (blue curve in **figure**). The overall gain of performances is not significantly different from the MFE predictions. However, for the sequences of length lesser than 200 nucleotides, this gain was found to be substantial and significant ($\approx 16\%$ better than the MFE). The accuracy for those sequences is equivalent to ML performances. For sequence lengths greater than 300 nucleotides, we observed the same drastic loss of accuracy, although we took only the best prediction among the 50 saved configurations for each sequence.

Two regions of lack of performances were observed for all methods. A group of 28 sequences of length shorter than 80 nucleotides were evaluated with free of their known structures about 9.8 kcal/mol greater than the MFE structures. Some of them involve large exterior loop such as displayed in **figure**. The second region is around 200 nucleotides length. The known structure of these sequences also displayed large unpaired regions such as the one shown in **figure**.

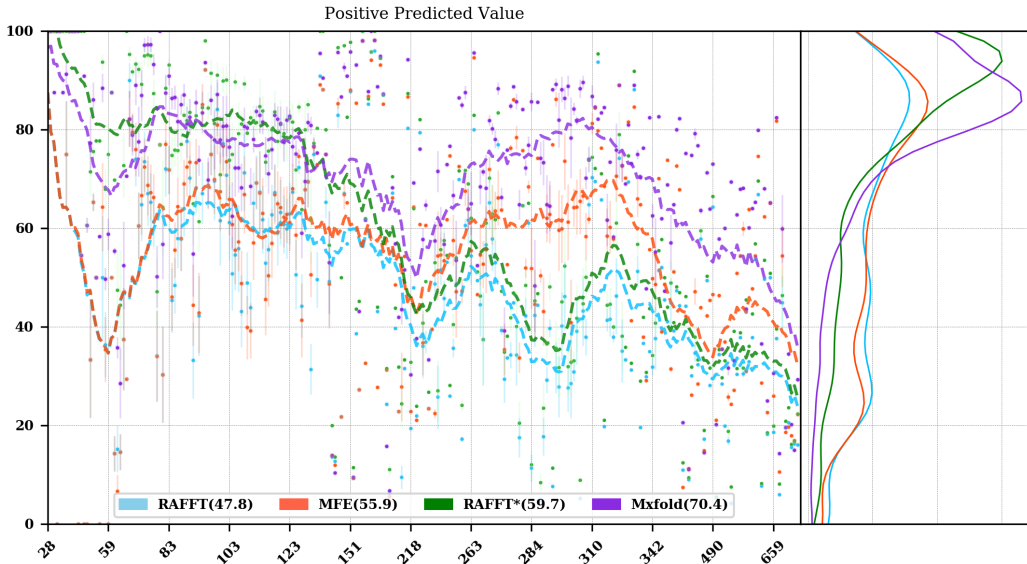


Figure 1: Folding comparison by taking the best energy among the 30 predicted trajectories

To investigate the region of the structure space where the thermodynamic model tends to fail, we computed the composition content of the known structures. **Figure** shows the percent of base pairs or positions involved in the five loop types: interior, exterior, hairpin, stacking, and multi-branch loops. Those percents were then represented in a principal component analysis.

From the PCA, we observed that the known structures are distributed in the structure space non-uniformly. Some natural structures, as observed above, have large exterior loops. The center of mass in the principal component space is located in between the high density stacking and interior loops. This shows that the dataset contains many elongated structures.

It shows that the MFE predictions tend to fail when the structure contains a high proportion of interior loops as shown in **figure**.

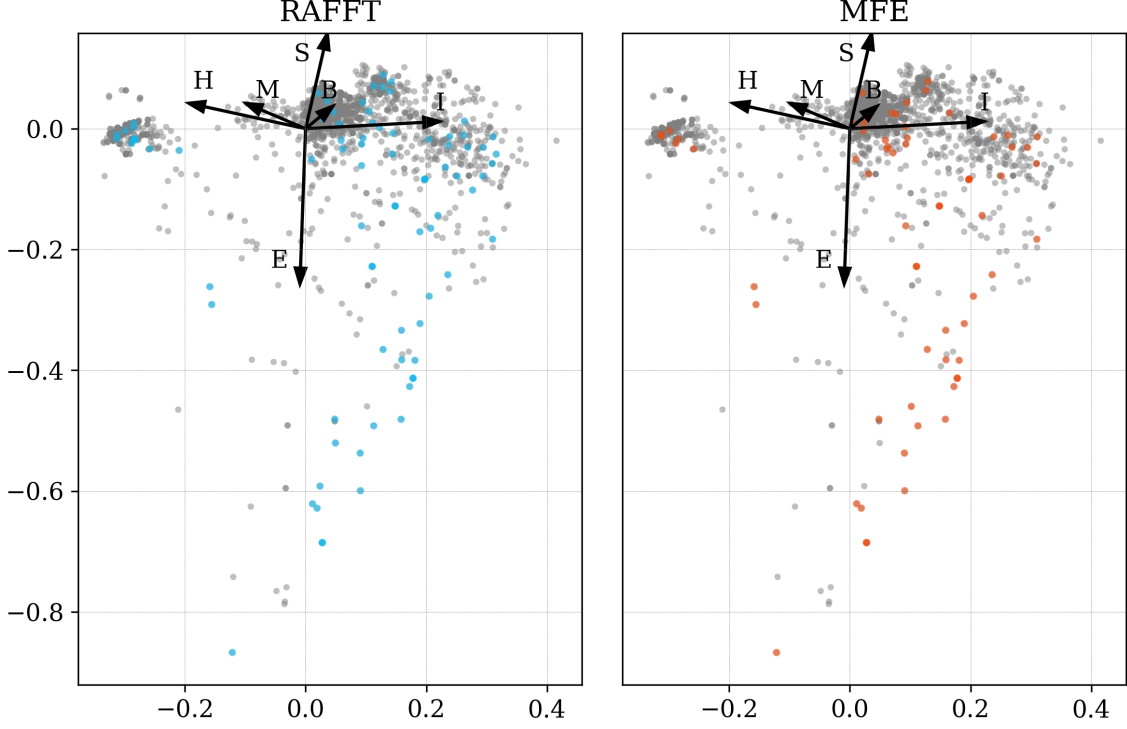


Figure 2: where does the methods failed? PCA RNAfold, Mxfold, FFT, and

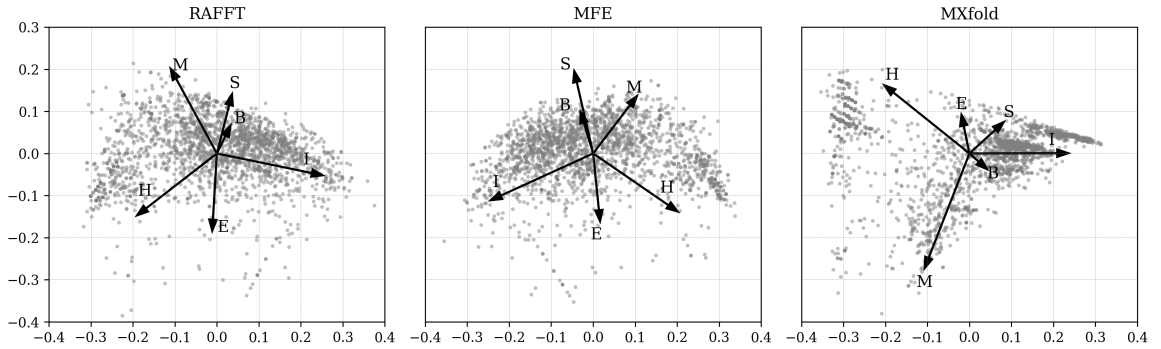


Figure 3: What kind of structure these method naturally produce

5 Methods

We formed two sub-datasets based on the ArchiveII (**ref**) dataset. First, we removed from all the structure containing pseudoknot since all tool considered here don't handle pseudoknots.

Next, we removed all the structures which were evaluated with a positive energy or null energy with the Turner 2004 energy parameters. Since positive energies means that the completely unfolded structure is more stable than the native one, we assume that those structures are not well modeled by the energy function used here. This dataset is composed of 2698 structures. 240 sequences were found multiple times (from 2 to 8 times). 19 of them were found with different structures. We discarded all duplication and picked the structure with the lowest energy for each. We obtained a dataset of 2296 sequences.

To compute the MFE structure, we used RNAfold (version) with the default parameters and the Turner 2004 set of energy parameters. For the machine learning tool, we computed the prediction using Mfold2 with the default parameters. The structures for both were used for the statistics.

For kinfold, we performed for each sequence, 40 simulations of 10^4 (unit?). Then, we counted the occurrences of each structures and selected the 50 most populated structures. The best structure in terms of PPV was displayed and used for the statistics.

For the FFT-based algorithm, we used two sets of parameters. First, we used search for consecutive base pairs in the 50 best modes and stored 50 conformations for which we displayed the best energy found. The correlation were computed using the weights $w_{GC}=3$, $w_{AU}=2$, and $w_{GU}=1$.

To measure the predictions accuracy, we used two metrics from epimiology. The positive predictive value (PPV) which is the fraction of correct base pairs predictions in the predicted structure. The sensitivity is the fraction of correctly predicted base pairs in the true structure. Both metrics are defined as follow:

$$PPV = \frac{TP}{TP + FN} \quad \text{Sensitivity} = \frac{TP}{TP + FP} \quad (5)$$

where TP, FN, and FP stand respectively for the number of correctly predicted base pairs (true positives), the number of base pairs not detected (false negatives), and the number of wrongly predicted base pairs (false positives). To maintain consistency with previous and future studies, we computed these metrics using the implementation in the **scorer** tool provided in **ref Mathews**, which provide also a more flexible estimate where shift are allowed.

The loop composition were extracted in terms of proportion to have an overall measure of the structure distribution. We first convert all natural structures into Shapiro notation using Vienna Package utilities. From the notation, we extracted the proportion of base pairs involved into the interior, exterior, bulge, stacking, and multibranch loops. For each true structure, we obtained a prcent of type of loops from which we extracted the principal components. Next, the structure compositions where projected on the first two principal components for visual conveniences. The composition arrows represents the eigen vectors obtained from the diagonalization of the covariance matrix.

6 Concluding discussion

6.1 Good stuff

1. Simple heuristic to compute folding path
2. Versatile method: allow simple modeling of pseudoknot and more information can be encoded in the mirror representation.
3. Performance is comparable although not as good as state of the art in the folding task.
4. One trajectory among the selected produce good structures (close with better accuracy than ML methods).

6.2 limits

1. Choosing the maximum number each time is not an optimal choice
2. In average, the scores are not good. Only a few out of the predicted structures have good scores.
3. The quality of the prediction degrade drastically when the size ≥ 250 from 74% \rightarrow 50%.
 - (a) The stacking method might one cause however, since MFE is degraded as well, we believe that it might partly explain by the thermodynamic model accuracy.
4. The distribution of loop types composition seems to differ between the Boltzmann ensemble and the natural structures.